Publishers B.V.: Amsterdam, 1991; pp 151-161. (b) Ohno, T.; Nozaki, K.; Ikeda, N.; Haga, M. In *Electron Transfer in Inorganic, Organic, and Biological Systems: Electron Transfer, Energy Transfer and Excited-State Annihilation in Binuclear Compounds of Ruthenium(II)*; Bolton, J. R., Mataga, N., McLendon, G., Eds.; Advances in Chemistry Series No. 228; American Chemical Society: Washington, DC, 1991; pp 215-228.
(24) Furue, M.; Hirata, M.; Kinoshita, S.; Kushida, T.; Kamachi, M. *Chem. Lett.* **1990**, 2065.
(25) O'Donnell, J. F.; Ayres, J. T.; Mann, C. K. *Anal. Chem.* **1965**, *37*, 1161.
(26) Britton, H. T. S.; Robinson, R. A. *J. Chem. Soc.* **1931**, *458*, 1456.
(27) Lay, P. A.; Sargeson, A.; Taube, H. *Inorg. Synth.* **1986**, *24*, 291.
(28) Haga, M.; Ano, T.; Ishizaki, T.; Kano, K.; Nozaki, K.; Ohno, T., submitted for publication.
(29) Nozaki, K.; Ohno, T.; Haga, M., to be published.
(30) Nozaki, K.; Oyama, M.; Hatano, H.; Okazaki, S. *J. Electroanal. Chem., Interfacial Electroanal.* **1989**, *270*, 191.
(31) Nomura, S.; Nozaki, K.; Okazaki, S. *Anal. Chem.* **1991**, *63*, 2665.
(32) Duyne, R. P. V.; Reilley, C. N. *Anal. Chem.* **1972**, *44*, 142.
(33) Sutton, J. E.; Sutton, P. M.; Taube, H. *Inorg. Chem.* **1979**, *18*, 1017.
(34) Nicholson, R. S.; Shain, I. *Anal. Chem.* **1964**, *36*, 706.
(35) Ballardini, R.; Varani, G.; Balzani, V. *J. Am. Chem. Soc.* **1980**, *102*, 1719.
(36) Indelli, M. T.; Carioli, A.; Scandola, F. *J. Phys. Chem.* **1984**, *88*, 2685.
(37) Nozaki, K.; Ohno, T.; Haga, M., to be published.
(38) Unpublished data.
(39) Creutz, C.; Keller, A. D.; Sutin, N.; Zipp, A. P. *J. Am. Chem. Soc.* **1982**, *104*, 3618.
(40) Lee, G.-H.; Ciara, L. D.; Haim, A. *J. Am. Chem. Soc.* **1989**, *111*, 2535.
(41) Gennett, T.; Milner, D. F.; Weaver, M. J. *J. Phys. Chem.* **1985**, *89*, 2787.
(42) Nielson, R. M.; McManis, G. E.; Golovin, M. N.; Weaver, M. J. *J. Phys. Chem.* **1988**, *92*, 3441.
(43) Calef, D. F.; Wolynes, P. G. *J. Phys. Chem.* **1983**, *87*, 3387.
(44) Hynes, J. I. *J. Phys. Chem.* **1986**, *90*, 3701.
(45) Sumi, H.; Marcus, R. A. *J. Chem. Phys.* **1986**, *84*, 4894.
(46) Rips, I.; Jortner, J. *J. Chem. Phys.* **1987**, *87*, 2090.
(47) Simon, J. D. *Acc. Chem. Res.* **1988**, *21*, 128.
(48) E_m = 0.047 meV (acetone); 0.043 meV (acetonitrile).[41]
(49) Riddick, J. A.; Bunger, W. B.; Sakano, T. K. *Organic Solvants, Physical Properties and Methods of Purification*; John Wiley: New York, 1986.
(50) Although the ET rates were measured in the mixed solvent of BN/PN (7:3), the dielectric relaxation time of the mixed solvent is difficult to be estimated. However, the frequency factor is probably almost the same as that in BN.
(51) From the condition for adiabatic ET ($\nu_{el} \gg 2\nu_n$), H_{rp} is calculated to be more than 7 meV using eq 4 and the parameters of $\nu_n = 3.9 \times 10^{11}$ s^{-1} and $\lambda = 1$ eV.
(52) Kestner, N.; Logan, J.; Jortner, J. *J. Phys. Chem.* **1974**, *78*, 2148.
(53) Ulstrup, J.; Jortner, J. *J. Chem. Phys.* **1975**, *63*, 4358.
(54) Brunschwig, B. S.; Logan, J.; Newton, M. D.; Sutin, N. *J. Am. Chem. Soc.* **1980**, *102*, 5798.
(55) (a) Levich, V. G.; Dogonadze, R. R. *Dokl. Acad. Nauk. SSSR* **1960**, *133*, 158. (b) Dogonadze, R. R. *Dokl. Acad. Nauk. SSSR* **1960**, *142*, 1108.
(56) Ohno, T.; Yoshimura, A.; Prasad, D. R.; Hoffman, M. Z. *J. Phys. Chem.* **1991**, *95*, 4723.
(57) Ohno, T. *J. Phys. Chem.* **1985**, *89*, 5709.
(58) Ohno, T.; Yoshimura, A.; Shioyama, H.; Mataga, N. *J. Phys. Chem.* **1987**, *91*, 4365.

Reactions of $Al^+(^1S)$ with NO_2, N_2O, and CO_2: Thermochemistry of AlO and AlO^+

D. E. Clemmer, M. E. Weber,† and P. B. Armentrout*,‡

Department of Chemistry, University of Utah, Salt Lake City, Utah 84112 *(Received: August 13, 1992; In Final Form: October 2, 1992)*

Cross sections as a function of reagent collision energy are measured for the reaction of $Al^+(^1S)$ with NO_2, N_2O, and CO_2 by using guided-ion-beam mass spectrometry. In the NO_2 system, $NO^+ + AlO$ and $AlO^+ + NO$ are formed in endothermic reactions. The threshold for the former reaction is used to measure the bond energy, $D°_0(AlO) = 123.1 \pm 1.0$ kcal/mol, in good agreement with the presently accepted value of 121.2 ± 2.2 kcal/mol [*J. Chem. Phys. Ref. Data* **1983**, *12*, 967]. Combining this bond energy with other thermochemistry gives the AlO ionization energy, $IE(AlO) = 9.82 \pm 0.13$ eV. The reactions of Al^+ with N_2O and CO_2 also form AlO^+, but the thresholds for these systems do not correspond with the thermodynamic limit. The origins of the activation barriers postulated to explain this behavior are discussed.

Introduction

Recent studies in our laboratory and others have investigated the reactivity of atomic metal ions with small molecules that contain oxygen atoms, such as O_2,[1-9] CO,[4,8,10,11] NO,[4,5,7,11] O_3,[4-7,11] CO_2,[4,7,8] NO_2,[12-15] N_2O,[3,4,9,11] and H_2O.[8,16] These studies are useful for determining the thermochemistry for metal-oxygen molecules, providing insight into the nature of the M-O bond and defining the fundamental requirements necessary for activating O-O, C-O, and N-O bonds. In this work, we continue these efforts by reporting the results for reactions of Al^+ with NO_2, N_2O, and CO_2. The only previous studies of these reactions are the work of Rutherford and Vroom, who examined the reaction of Al^+ with N_2O using a crossed-ion modulated-neutral-beam apparatus.[3]

Aside from the fundamental importance of building an accurate thermochemical data base for metal-oxygen bonds, studies of the thermochemistry of AlO are also motivated by the possible environmental importance of this molecule.[17] It is possible that Al (which is deposited into the stratosphere in considerable quantities by rocket engines) might participate in an ozone-destruction cycle[18,19] by reactions 1 and 2. Because $D°_0(AlO)$ is much larger

$$Al + O_3 \rightarrow AlO + O_2 \quad (1)$$

$$O + AlO \rightarrow Al + O_2 \quad (2)$$

than $D°_0(O_2\text{-}O) = 24.2$ kcal/mol,[20] reaction 1 is likely to proceed fairly efficiently. Further, if $D°(AlO)$ is less than or close to $D°_0(O_2) = 118$ kcal/mol,[20] then reaction 2 can regenerate Al such that the net reaction results in a catalytic depletion of ozone.

A critical and comprehensive assessment of the welter of thermochemical measurements involving AlO is beyond the scope of this paper. Fortunately, the studies reported prior to 1983 have been assessed in detail by Pedley and Marshall.[25] They conclude that $D°_0(AlO) = 121.2 \pm 2.2$ kcal/mol is the best value for the neutral bond energy based mainly on the chemiluminescence and laser fluorescence studies of Zare and co-workers[21] and Pasternack and Dagdigian[22] that were reported in the late 1970s. However, this thermochemistry is not without question. There is a group of measurements that lies below this value, near 118 kcal/mol,[25] and another group of values near 126 kcal/mol.[17,25] Further, one of these higher values came from experiments that followed the

† Present address: NASA, Lyndon B. Johnson Space Center, Astronaut Office, Houston, TX 77058.
‡ Camille and Henry Dreyfus Teacher-Scholar, 1987-1992.

0022-3654/92/2096-10888$03.00/0 © 1992 American Chemical Society

TABLE I: Literature Thermochemistry at 0 K

MX	$D°_0$(MX),[a] kcal/mol	IE(MX), eV
ON–O	71.85 (0.20)	
N–O	150.06 (0.05)	9.264 36 (0.000 06)
O_2	117.97 (0.03)	
OC–O	125.75 (0.05)	
C–O	256.16 (0.12)	
N_2–O	38.55 (0.10)	
Al		5.985 7708 (0.000 0004)[b]
AlO	121.2 (2.2)[c]	
	123.1 (1.0)[d]	9.82 (0.13)[d,e]
Al^+–O	34.6 (2.8)[f]	

[a] All bond energies are calculated using the thermochemistry in ref 20 unless otherwise noted. [b] Chang, E. S. *J. Phys. Chem. Ref. Data* **1990**, *19*, 119. [c] Value recommended by Pedley and Marshall (ref 25). [d] This work. [e] Calculated by using eq 15. [f] Reference 1.

chemiluminescence and laser fluorescence studies and, therefore, was aware of, but could not rationalize, the differences.[17]

The thermochemistry for AlO^+ is not as extensively studied as that for AlO. In 1986, measurements of the endothermicity of reaction 3 made in our laboratory were used to determine a

$$Al^+ + O_2 \rightarrow AlO^+ + O \quad (3)$$

lower limit for the Al^+–O bond energy of 34.6 ± 2.8 kcal/mol.[1] The bond energy was assigned as a lower limit at that time because the limitations associated with measuring accurate thermochemistry by guided-ion-beam mass spectrometry were still being evaluated and because it is impossible to rule out a reaction barrier. Our limit was slightly lower than but within experimental error of $D°(Al^+–O)$ = 39.5 ± 4.1 kcal/mol calculated from $D°_0(AlO)$ = 121.2 ± 2.2 kcal/mol and the AlO ionization energy measured by Hildebrand, 9.53 ± 0.15 eV.[23] Since this work, we have studied a large number of reactions analogous to reaction 3.[2] This work suggests that the thermochemistry obtained from the O_2 system is accurate. For the purposes of this paper, we also reanalyzed our original $Al^+ + O_2$ data using techniques that have now been tested on a large number of systems. This new analysis is in complete agreement with the original interpretation of the data. We now believe that our previously reported limit for the Al^+–O bond energy is likely to be an equality. This interpretation demands that either the ionization energy measured by Hildenbrand or the AlO bond energy recommended by Pedley and Marshall is inaccurate.

The present work allows us to carefully test both of these possibilities. The thermochemistry for AlO is determined by studying the reaction of Al^+ with NO_2. Reactions of atomic metal ions with NO_2 are particularly useful in obtaining information about the gas-phase thermochemistry of neutral and cationic metal oxides because the ON–O bond is weak, $D°_0(ON–O)$ = 71.85 ± 0.20 kcal/mol,[20] Table I, and the NO fragment has a relatively low ionization energy IE(NO) = 9.264 36 ± 0.000 06 eV.[24] Thus, reactions analogous to those studied here, processes 4 and 5, occur

$$Al^+ + NO_2 \rightarrow AlO^+ + NO \quad (4)$$

$$Al^+ + NO_2 \rightarrow NO^+ + AlO \quad (5)$$

readily. To date, we have used the NO_2 system to measure thermochemistry for most of the first-row transition-metal oxide diatomics,[12,13] several diatomic metal oxides of the second row,[15] and the group 3 dioxides (ScO_2, YO_2, and LaO_2).[14] In cases where accurate thermochemistry is available in the literature (such as FeO, CoO, NiO, and CuO),[25] our results are in good agreement, giving us confidence in the accuracy of the thermochemistry obtained from the $M^+ + NO_2$ system.

Studies of the reactions of Al^+ with N_2O and CO_2, processes 6 and 7, were also performed to help verify the AlO^+ thermochemistry. Although we find that neither of these systems provides

$$Al^+ + N_2O \rightarrow AlO^+ + N_2 \quad (6)$$

$$Al^+ + CO_2 \rightarrow AlO^+ + CO \quad (7)$$

useful thermochemical information, the reasons for this and the dynamics of these reactions are of interest.

TABLE II: Spin and Orbital Angular Momentum Correlations

reactants	products	$\Delta\Sigma$[a]	$\Delta\Lambda$[b]
$Al^+(^1S) + O_2(^3\Sigma_g^-)$	$AlO^+(^3\Pi) + O(^3P)$	0, ±1	0, ±1, ±2
	$AlO^+(^1\Sigma^+) + O(^3P)$	0	0, ±1
$Al^+(^1S) + NO_2(^2A_1)$	$AlO(^2\Sigma^+) + NO^+(^1\Sigma^+)$	0	
	$AlO^+(^3\Pi) + NO(^2\Pi)$	0, ±1	
	$AlO^+(^1\Sigma^+) + NO(^2\Pi)$	0	
$Al^+(^1S) + N_2O(^1\Sigma^+)$	$AlO^+(^3\Pi) + N_2(^1\Sigma_g^+)$	±1	±1
	$AlO^+(^1\Sigma^+) + N_2(^1\Sigma_g^+)$	0	0
$Al^+(^1S) + CO_2(^1\Sigma_g^+)$	$AlO^+(^3\Pi) + CO(^1\Sigma^+)$	±1	±1
	$AlO^+(^1\Sigma^+) + CO(^1\Sigma^+)$	0	0

[a] Changes in the spin quantum number in going from reactants to products. [b] Changes in the orbital angular momentum quantum number in going from reactants to products.

Potential Energy Surfaces

One of the complexities of reactions 3, 4, 6, and 7 is that there are several low-lying states of AlO^+. While no experimental data are available, calculations by Schamps predict a ground state of $^3\Pi$, a $^1\Sigma^+$ state that lies 0.04 eV higher in energy, and a $^1\Pi$ state at 0.28 eV.[26] The accuracy of these calculations, ~0.1 eV, does not definitively predict whether the $^3\Pi$ state or the $^1\Sigma^+$ state is the true ground state. To determine which state can be produced in the reactions of Al^+ with O_2, NO_2, N_2O, and CO_2, we first consider whether spin and orbital angular momentum can be conserved in these reactions. Table II shows the ground states of the reactants and products for these four systems. This table also lists how the quantum numbers for spin, Σ, and orbital angular momentum, Λ, can change in going from reactants to products. As previously discussed for the O_2 system,[1] spin and orbital angular momentum can both be conserved in reaction 3 whether the $^3\Pi$ state or the $^1\Sigma^+$ state of AlO^+ is formed. In the NO_2 system, Λ is not a good quantum number; however, spin is conserved for both reactions 4 and 5. Reactions 6 and 7 can only conserve spin and orbital angular momentum if $AlO^+(^1\Sigma^+)$ is formed. Coupling between the spin and orbital angular momentum could permit formation of $AlO^+(^3\Pi)$ to take place, although such coupling is not expected to be very important in these light atom systems.

Another way to consider the potential energy surfaces of these reactions is to examine the correlations with separated atoms. In the O_2 system, the ground-state-separated atom limit is $Al^+(^1S)$ + $2O(^3P)$, and this correlates with ground-state reactants and $AlO^+(^3\Pi) + O(^3P)$ products. The $AlO^+(^1\Sigma^+) + O(^3P)$ products correlate with an excited separated atom asymptote, $Al^+(^1S)$ + $O(^3P) + O(^1D)$, 1.97 eV higher in energy than the ground-state asymptote.[27] Thus, reaction 3 is expected to favor the formation of the diabatically allowed $AlO^+(^3\Pi)$ product. In the NO_2 system, the situation is similar in that the separated dissociation limit has a ground state of $Al^+(^1S) + O(^3P) + NO(^2\Pi)$ that correlates with ground-state reactants and $AlO^+(^3\Pi) + NO(^2\Pi)$ products. Thus, reaction 4 is also expected to favor production of AlO^+ in its $^3\Pi$ state. In the N_2O and CO_2 systems, the ground-state-separated dissociation products, $Al^+(^1S) + O(^3P) + N_2(^1\Sigma_g^+)$ and $Al^+(^1S)$ + $O(^3P) + CO(^1\Sigma^+)$, correlate with the $AlO^+(^3\Pi)$ product and with highly excited triplet states of the N_2O and CO_2 reactants. Ground-state reactants, $Al^+(^1S) + N_2O(^1\Sigma^+)$ and $Al^+(^1S)$ + $CO_2(^1\Sigma_g^+)$, correlate with $Al^+(^1S) + O(^1D) + N_2(^1\Sigma_g^+)$ and $Al^+(^1S) + O(^1D) + CO(^1\Sigma^+)$, which correlates with $AlO^+(^1\Sigma^+)$ + $N_2(^1\Sigma_g^+)$ and $AlO^+(^1\Sigma^+) + CO(^1\Sigma^+)$ products. Here, the correlations suggest that reactions 6 and 7 will favor the formation of AlO^+ in its $^1\Sigma^+$ state.

Experimental Section

General. Complete descriptions of the apparatus and experimental procedures are given elsewhere.[28] For the reaction with NO_2, Al^+ ions were produced by argon ion bombardment of an aluminum rod in a dc-discharge/flow-tube (FT) source (described previously).[29] The Al^+ ions undergo ~10^5 collisions with the Ar/He buffer gas mixture before exiting the flow tube. This thermalizes the ions such that they are expected to be exclusively

TABLE III: Summary of Parameters of Equation 8 Used To Model Cross Sections[a]

reaction	E_0, eV	σ_0	n	E_D,[b] eV
4	1.75 (0.06)	10.7 (0.7)	1.3 (0.2)	
5	1.05 (0.05)	41.3 (4.1)	0.7 (0.1)	1.83 (0.10)
6	0.82 (0.10)	1.57 (0.35)	1.4 (0.2)	≡1.67
7	5.33 (0.20)	0.10 (0.04)	2.2 (0.4)	

[a] Uncertainties in parentheses. [b] The parameter p in the high-energy model described in ref 1 is 0.0 for reactions 5 and 6.

in the ^1S ground electronic state. For the reactions with N_2O and CO_2, Al^+ ions were generated by surface ionization at a filament temperature of ~2100 K of vaporized $AlCl_3$ or AlF_3, as described previously.[1] Assuming that the ions equilibrate at the temperature of the source, we calculate that >99.99% of the Al^+ ions are in the ^1S ground state. No evidence for excited ions is observed in this study for ions produced in either source.

The ions are extracted from the source, accelerated, and focused into a magnetic sector momentum analyzer for mass analysis. Mass-selected ions are slowed to a desired kinetic energy and focused into an octopole ion trap. This device guides the ions through a static gas cell containing a low pressure (0.01–0.30 mTorr) of NO_2 (purified as described before),[12] N_2O, or CO_2 reagents. After exiting the gas cell, product and unreacted beam ions drift to the end of the octopole where they are directed into a quadrupole mass filter for mass analysis and then detected by using a secondary electron scintillation detector and pulse-counting electronics. Conversion of raw ion intensities into reaction cross sections and the calibration of the absolute energy scale are treated as described previously.[28] Uncertainties in the cross sections are estimated to be ±20%. The beams are found to have a Gaussian kinetic energy distribution with a FWHM of ~0.3 eV in the laboratory frame. Uncertainties in the absolute energy scale are ±0.05-eV lab. All product cross sections reported are the results of single-ion-molecule collisions as verified by examining the pressure dependence of the product intensities.

Threshold Analysis. Previous work[2,10,30,31] has shown that cross sections for endothermic reactions can be analyzed by using eq 8, where σ_0 is a scaling factor, E is the relative kinetic energy,

$$\sigma(E) = \sigma_0(E - E_0 + E_{vib} + E_{rot})^n/E \quad (8)$$

n is an adjustable parameter, and E_0 is the 0 K threshold for reaction of ground electronic, vibrational, and rotational state reactants. In this study, E_{vib} represents the average vibrational energy of NO_2 (0.003 eV), N_2O (0.010 eV), and CO_2 (0.008 eV)[32] at 305 K (the nominal temperature of the octopole) and E_{rot} is the total rotational energy of NO_2 ($3kT/2$ = 0.039 eV), N_2O, or CO_2 (kT = 0.026 eV). In order to model the high-energy portion of the cross sections, we use a modified form of eq 8 (discussed previously)[1] that accounts for a decline in the product ion cross section above an energy E_D where a dissociation channel or competing reaction can begin.

Before comparison with the experimental data, eq 8 is convoluted with the neutral and ion kinetic energy distributions as described previously.[28] The σ_0, n, E_0, and E_D parameters are then optimized by using a nonlinear least-squares analysis to give the best reproduction of the data. Error limits for E_0 are calculated from the range of threshold values obtained for different data sets with different values of n and the uncertainty in the absolute energy scale. The resulting parameters found upon this treatment of the cross sections are given in Table III. Overall, eq 8 and its modified form accurately reproduce all of the data discussed here.

Results

$Al^+ + NO_2$. Two ionic products, AlO^+ and NO^+, are formed in the reaction of Al^+ with NO_2 and correspond to reactions 4 and 5. The cross sections for these processes are shown in Figure 1. Both reactions are clearly endothermic, and NO^+ formation is favored at all energies. There is no ambiguity that the neutral product of reaction 5 is AlO since the threshold for producing

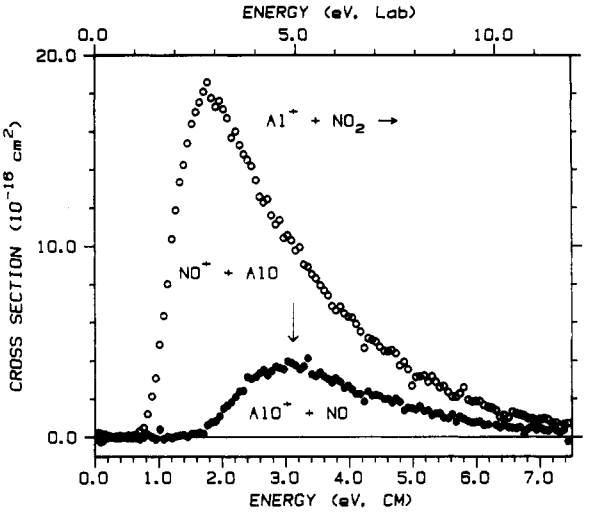

Figure 1. Variation of product cross sections for the formation of AlO^+ (solid circles) and NO^+ (open circles) from the reaction of Al^+ with NO_2 as a function of kinetic energy in the center-of-mass frame (lower axis) and the laboratory frame (upper axis). The arrow indicates the bond energy of NO_2 at 3.116 eV.

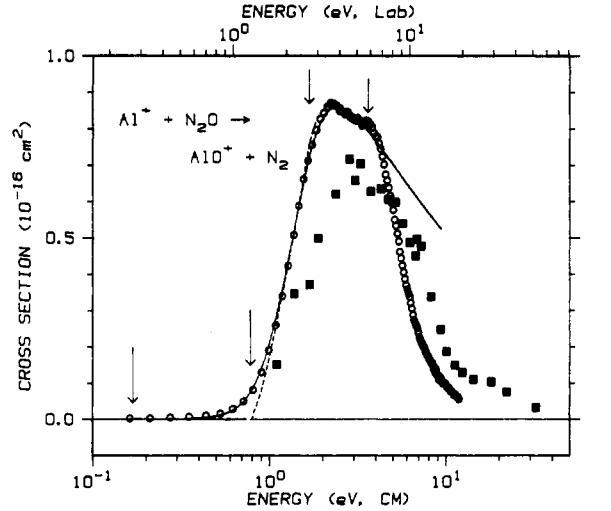

Figure 2. Cross section for the formation of AlO^+ from reaction of Al^+ with N_2O as a function of kinetic energy in the center-of-mass frame (lower axis) and the laboratory frame (upper axis). Open circles show the present results, and solid squares show the results of Rutherford and Vroom, ref 3. The dashed line shows the model cross section given by eq 8 and the parameters given in Table III. The full line shows this model convoluted with the experimental energy distributions. Arrows indicate the calculated threshold for reaction 6 at 0.17 eV, the measured threshold of 0.82 eV, the bond energy of N_2O at 1.67 eV, and the dissociation asymptote to form $O(^1D)$ at 3.64 eV.

$NO^+ + Al + O$ is ~6.4 eV (Table I), much higher than the observed threshold.

The cross section for the formation of $NO^+ + AlO$ reaches a maximum at about 1.8 eV, very close to the apparent threshold for the formation of $AlO^+ + NO$. This implies a strong competition between reactions 4 and 5, which seems reasonable because the products of these reactions differ only in the location of the charge. There might also be additional constraints on the magnitude of the total cross section because the decline in $\sigma(NO^+)$ is greater than the increase in $\sigma(AlO^+)$. Indeed, the calculated collision cross section[33] is of the same order of magnitude as the total cross section in this energy region, although the utility of this calculated cross section at such high kinetic energies is not clear.

The cross section for reaction 4 peaks near $D°_0(ON–O)$ = 3.116 eV.[20] This shows that the AlO^+ product dissociates above this energy by an overall process that corresponds to reaction 9.

$$Al^+ + NO_2 \rightarrow Al^+ + O + NO \quad (9)$$

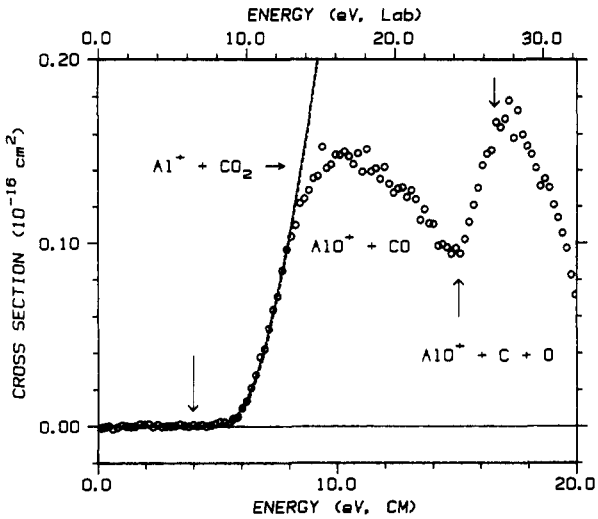

Figure 3. Cross section for the formation of AlO^+ from the reaction of Al^+ with CO_2 (open circles) as a function of kinetic energy in the center-of-mass frame (lower scale) and laboratory frame (upper scale). The dashed line shows the model cross section given by eq 8 and the parameters given in Table II. The full line shows this model convoluted with the experimental energy distributions. Arrows indicate the calculated threshold for reaction 7 at 3.95 eV, the calculated threshold for reaction 13 at 15.06 eV, and the atomization energy for the system of 16.56 eV. The measured threshold is at 5.33 eV.

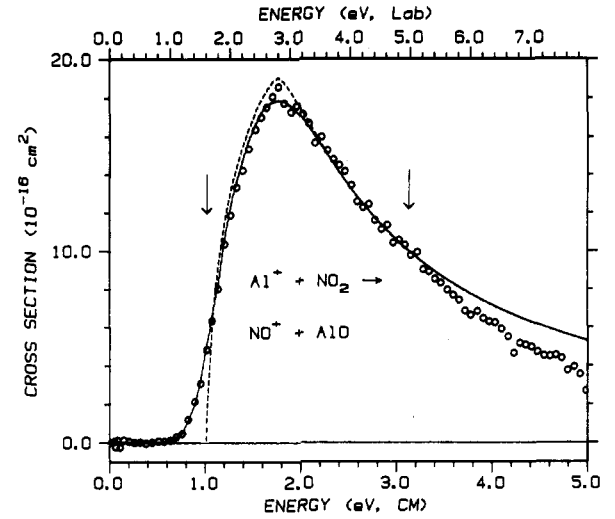

Figure 4. Cross section for the formation of $NO^+ + AlO$ from the reaction of $Al^+ + NO_2$ (open circles) as a function of kinetic energy in the center-of-mass frame (lower scale) and laboratory frame (upper scale). The dashed line shows the model cross section given by eq 8 and the parameters given in Table III. The full line shows this fit convoluted with the experimental energy distributions. Arrows indicate the threshold energy at 1.05 eV and the NO_2 bond energy of 3.116 eV.

$Al^+ + N_2O$. The major ionic product observed in the reaction of Al^+ with N_2O is AlO^+, formed in reaction 6. The cross sections for this process are displayed in Figure 2 and are consistent with the previous results of Rutherford and Vroom,[3] which are also shown.

The thermodynamic threshold for AlO^+ formation in reaction 6 can be calculated by using the thermochemistry given in Table I and eq 10, where $D°_0(X–O)$ is the energy of the $N_2–O$ bond

$$E_0 = D°_0(X–O) - D°_0(Al^+–O) \quad (10)$$

that is broken. This yields $E_0 = 0.17 \pm 0.12$ eV, which is below the 0.4-eV apparent threshold for this cross section. The AlO^+ cross section peaks near $D°_0(N_2–O) = 38.6$ kcal/mol (1.67 eV), suggesting that the AlO^+ product begins to dissociate at the threshold for the overall reaction (11). The reason for the rapid

$$Al^+(^1S) + N_2O(^1\Sigma^+) \rightarrow Al^+(^1S) + O(^3P) + N_2(^1\Sigma_g^+) \quad (11)$$

decline in this cross section at energies above 4 eV is not completely clear but may be associated with the dissociation channel reaction (12), which can begin at 3.64 eV. This suggestion is consistent

$$Al^+(^1S) + N_2O(^1\Sigma^+) \rightarrow Al^+(^1S) + O(^1D) + N_2(^1\Sigma_g^+) \quad (12)$$

with the discussion above that reaction 6 is likely to form $AlO^+(^1\Sigma^+)$, which dissociates diabatically to $Al^+(^1S) + O(^1D)$. The observation that the AlO^+ cross section declines slowly at the threshold for reaction 11 and then much more rapidly once process 12 is energetically allowed may indicate either that AlO^+ is formed in both its $^3\Pi$ and $^1\Sigma^+$ states (with the latter state dominating) or that it is formed predominantly or exclusively in the $^1\Sigma^+$ state, which can dissociate slowly to $Al^+(^1S) + O(^3P)$ via a singlet–triplet surface crossing and rapidly to $Al^+(^1S) + O(^1D)$ along a spin-allowed pathway.

A final note about the $Al^+ + N_2O$ system is that formation of AlO_2^+ is also observed. The energy dependence of this species and pressure-dependent studies verify that this is due to a secondary reaction between the primary AlO^+ product and N_2O. The efficiency of this process indicates that this secondary reaction is probably exothermic. This observation indicates that $D°(OAl^+–O) > D°(N_2–O) = 38.6$ kcal/mol, which is consistent with $D°(OAl^+–O) = 76 \pm 24$ kcal/mol.[34,35]

$Al^+ + CO_2$. AlO^+ formation is also the major product observed in the reaction of $Al^+ + CO_2$, reaction 7. The cross section for this process is shown in Figure 3. Using eq 10 and the thermochemistry given in Table I, we calculate that reaction 7 can begin at 3.95 ± 0.12 eV. As in the N_2O system, the apparent threshold for AlO^+ formation from reaction 7 is above the thermodynamic value, near 5 eV.

The AlO^+ cross-section behavior in this system is complex, displaying two distinct features. The second feature becomes noticeable near 15 eV, which corresponds closely with the 15.06 ± 0.12 eV threshold for process 13. This second feature then

$$Al^+ + CO_2 \rightarrow AlO^+ + C + O \quad (13)$$

reaches a maximum near 17 eV, close to the atomization energy of CO_2, 16.561 ± 0.005 eV. This observation suggests that a significant fraction of the available translational energy is converted into internal energy of CO_2 during the collision.

Discussion

$Al^+ + NO_2$ Data Analysis. The data for reaction 5 are analyzed with eq 8 as discussed above. At higher energies, above $E_D = 1.8$ eV, the competition with reaction 4 is included in the model. The average of the optimized parameters for five data sets is given in Table III, and this average model is compared with a single data set in Figure 4. Clearly, the model does an excellent job of representing the data from threshold to 3.1 eV, where reaction 9 can begin. This deviation is evidence that reaction 9 competes with the formation of both NO^+ and AlO^+ and further supports the idea that these product channels are tightly coupled.

If there are no energy barriers in excess of the reaction endothermicity, as is often true for endothermic ion–molecule reactions,[31,36] then the threshold energy for reaction 5 can be equated with the reaction enthalpy. Thus, we can calculate $D°_0(Al–O)$ by using eq 14. Table III is combined with the thermochemistry

$$D°_0(Al–O) = D°_0(ON–O) + IE(NO) - IE(Al) - E_0(5) \quad (14)$$

given in Table I, we determine $D°_0(AlO) = 123.1 \pm 1.0$ kcal/mol, in agreement with $D°(AlO) = 121.2 \pm 2.2$ kcal/mol recommended by Pedley and Marshall.[25] From a practical viewpoint, it is comforting that the current value exceeds $D°_0(O_2)$, since this means that reaction 2 is endothermic. This implies that aluminum is unlikely to play a significant role in ozone destruction, although reaction 1, exothermic by 98.7 kcal/mol, could form internally excited AlO, which could react efficiently with oxygen atoms in process 2.

The cross section for AlO^+ formed in the reaction of Al^+ with NO_2 was also analyzed by using eq 8. The optimized parameters are given in Table III. The measured threshold of 1.75 ± 0.06

eV is within experimental error of $E_0 = 1.61 \pm 0.12$ eV calculated from the thermochemistry given in Table I. This helps verify that the bond energy measured from reaction 3 is accurate. We believe that the result obtained from our previous work is the best available because of the effects of competition between $AlO^+ + NO$ formation and the more favorable production of $NO^+ + AlO$. Such competition can lead to a slower rise in the cross section of the higher energy channel (consistent with the higher value of n for reaction 4 vs that for reaction 5, Table III), leading to a measured threshold conservatively viewed as an upper limit.

One final piece of thermodynamic information that comes from this work is the ionization energy of AlO, which is obtained by combining the neutral and ionic bond energies in eq 15. This

$$IE(AlO) = D°_0(AlO) - D°_0(Al^+–O) + IE(Al) \quad (15)$$

gives the value $IE(AlO) = 9.82 \pm 0.13$ eV, which is in good agreement with the value $IE(AlO) = 10.1 \pm 0.1$ eV obtained from SCF calculations by Schamps[26] and several less precise experimental values, 9.5 ± 1.0,[37] 10.3 ± 1.0,[38] and 9.9 ± 0.5 eV.[39] Our ionization energy is somewhat higher than the electron impact appearance energy measurements over alumina at temperatures of ≈2200–2300 K reported by Ho and Burns, 9.5 ± 0.2 eV,[35] and Hildebrand, 9.53 ± 0.15 eV.[23] The discrepancy between our value for IE(AlO) and these results is probably explained by the high-temperature source of AlO. This can easily cause hot bands that lead to an anomalously low value for the ionization energy.[1] Indeed the average internal energy of AlO at 2200 K is 0.39 eV.[40]

Another way of thinking about the present data is to realize that the difference in the thresholds of reactions 4 and 5 is the difference in the ionization energies of AlO and NO. If IE(AlO) were 9.53 ± 0.15 eV, the difference in the thresholds would be 0.27 ± 0.15 eV, while $IE(AlO) = 9.82 \pm 0.13$ eV yields a threshold difference of 0.56 ± 0.13 eV. The latter is within experimental error of the difference measured here of 0.70 ± 0.08 eV, Table III. (Again this value may be inflated slightly due to the competition between reactions 4 and 5.) Overall, if the threshold difference were as small as 0.27 eV, we would expect that the $AlO^+ + NO$ channel would compete more favorably with the $NO^+ + AlO$ channel than the data of Figure 1 show.

$Al^+ + N_2O$ and CO_2 Data Analysis. Analysis of the cross sections for reactions 6 and 7 with eq 8 yields the optimized parameters given in Table III. The measured thresholds of 0.82 ± 0.10 and 5.33 ± 0.20 eV, respectively, are considerably above the thremodynamic thresholds calculated from the literature thermochemistry, 0.17 ± 0.12 and 3.95 ± 0.12 eV. Since there are no other competing primary reactions in these systems, there are two possible explanations for these results. First, as discussed above, reactions 6 and 7 are likely to form $AlO^+(^1\Sigma^+)$ rather than $AlO^+(^3\Pi)$, which is believed to be generated in reactions 3 and 4. Thus, the thresholds measured here could correspond to the thermodynamic thresholds for this excited state of AlO^+. However, this interpretation of the data yields different excitation energies in the two systems, 0.65 ± 0.16 eV from N_2O and 1.38 ± 0.23 eV from CO_2, and both values are well above the calculated value of 0.04 eV.[26] Therefore, the more likely explanation is the second possibility that these reactions have barriers along the potential surface for AlO^+ formation.

Reaction barriers have been observed for the reaction of atomic transition-metal ions with N_2O and their origins discussed previously.[9] A similar barrier has recently been observed in the photoinduced formation of VO^+ from $V(CO_2)^+$.[41] Since CO_2 and N_2O are isoelectronic, we expect that the barriers measured here have similar origins that are related to the potential energy surfaces discussed earlier in this paper. Because the ground states of $N_2O(^1\Sigma^+)$ and $CO_2(^1\Sigma_g^+)$ correlate with the excited dissociation products, $N_2(^1\Sigma_g^+) + O(^1D)$ and $CO(^1\Sigma^+) + O(^1D)$, respectively, thermal dissociation of N_2O (and presumably CO_2, although this has not been studied due to the very high temperatures required)[42] proceeds over a large activation barrier.[43,44] When $Al^+(^1S)$ interacts with these molecules to remove an oxygen atom, the singlet–triplet surface crossing in the isolated molecules will be perturbed. Complicating the story is the fact that AlO^+ can be formed either by crossing to the triplet surface to generate $AlO^+(^3\Pi)$ or by remaining on a singlet surface to form $AlO^+(^1\Sigma^+)$. The observation of barriers to reactions 6 and 7 suggests that whichever pathway is favored at the lowest energies, there is a bottleneck to the reaction that is probably associated with the singlet–triplet surface crossing in the isolated N_2O and CO_2 molecules.

The observation that no barrier is observed for reaction 13 is consistent with these ideas since dissociation of CO_2 to $C(^3P) + 2O(^3P)$ does not have any restrictions due to spin conservation. Thus, the efficiency of this process is similar to that of reaction 7, despite being 11 eV more endothermic. With this in mind, one might also expect to observe a similar feature in the AlO^+ cross section due to reaction 16. The threshold for reaction 16 and

$$Al^+ + N_2O \rightarrow AlO^+ + 2N \quad (16)$$

the atomization energy of N_2O are calculated to be 10.04 and 11.45 eV, respectively; however, neither we nor Rutherford and Vroom observe any obvious increase in the cross section in this energy range, Figure 2. It is possible that the cross section for reaction 16 is too small to be easily observed on top of that for reaction 6 (which is much larger than that for reaction 7) or that the $N(^4S)$ products do not lift the spin and orbital angular momentum restrictions to this process.

Conclusion

As discussed in the Introduction, literature information on the thermochemistry of AlO and AlO^+ is inconsistent. By examining the endothermic formation of $AlO + NO^+$ from $Al^+(^1S) + NO_2$, we are able to determine an AlO bond energy at 0 K of 123.1 ± 1.0 kcal/mol, in excellent agreement with the critically evaluated value of 121.2 ± 2.2 kcal/mol.[25] In the same system, the threshold for production of $AlO^+ + NO$ yields an AlO^+ bond energy consistent with $D°_0(Al^+–O) = 34.6 \pm 2.8$ kcal/mol, derived from previous work in our laboratory on the reaction of $Al^+(^1S) + O_2$.[1] Our recommended thermochemistry leads to an AlO ionization energy of 9.82 ± 0.13 eV, a value that suggests that the inconsistent thermochemistry in the literature is the result of ionization energies that are too low due to hot bands.

Reactions of Al^+ with N_2O and CO_2 were also studied in an effort to further confirm the thermochemistry for AlO^+. Although this species is produced in both systems, the thresholds measured for these processes are distinctly above the calculated thermodynamic values. An analysis of these systems suggests that these activation barriers are probably associated with the fact that processes that remove a ground-state oxygen atom from N_2O and CO_2 are not spin-allowed processes.

Acknowledgment. This work is supported by the National Science Foundation, Grant No. CHE-8917980.

References and Notes

(1) Weber, M. E.; Elkind, J. L.; Armentrout, P. B. *J. Chem. Phys.* **1986**, *84*, 1521.
(2) Fisher, E. R.; Elkind, J. L.; Clemmer, D. E.; Georgiadis, R.; Loh, S. K.; Aristov, N.; Sunderlin, L. S.; Armentrout, P. B. *J. Chem. Phys.* **1990**, *90*, 2676.
(3) Rutherford, J. A.; Vroom, D. A. *J. Chem. Phys.* **1976**, *65*, 4445.
(4) Kappes, M. M.; Staley, R. H. *J. Phys. Chem.* **1981**, *85*, 942.
(5) Johnsen, R.; Castell, F. R.; Biondi, M. A. *J. Chem. Phys.* **1975**, *61*, 5404.
(6) Ferguson, E. E.; Fehsenfeld, F. C. *J. Geophys. Res., Space Phys.* **1968**, *73*, 6215.
(7) Dheandhanoo, S.; Chatterjee, B. K.; Johnsen, R. *J. Chem. Phys.* **1985**, *83*, 3327.
(8) Armentrout, P. B.; Beauchamp, J. L. *Chem. Phys.* **1980**, *50*, 27.
(9) Armentrout, P. B.; Halle, L. F.; Beauchamp, J. L. *J. Chem. Phys.* **1982**, *76*, 2449.
(10) Clemmer, D. E.; Elkind, J. L.; Aristov, N.; Armentrout, P. B. *J. Chem. Phys.* **1991**, *95*, 3387.
(11) Rowe, B. R.; Fahey, D. W.; Ferguson, E. E.; Fehsenfeld, F. C. *J. Chem. Phys.* **1981**, *75*, 3325.
(12) Clemmer, D. E.; Dalleska, N. F.; Armentrout, P. B. *J. Chem. Phys.* **1991**, *95*, 7263.
(13) Clemmer, D. E.; Dalleska, N. F.; Loh, S. K.; Armentrout, P. B. Work in progress.
(14) Clemmer, D. E.; Dalleska, N. F.; Armentrout, P. B. *Chem. Phys. Lett.* **1992**, *190*, 259.

(15) Chen, Y.-M.; Armentrout, P. B. Work in progress.
(16) Clemmer, D. E. Ph.D. Thesis, University of Utah, 1992.
(17) Fontijn, A.; Felder, W. *J. Chem. Phys.* **1979**, *71*, 4854.
(18) Johnston, H. S. *Science* **1971**, *173*, 517.
(19) Dotto, L.; Schiff, H. I. *The Ozone War*; Doubleday: New York, 1978.
(20) Chase, M. W.; Davies, C. A.; Downey, J. R.; Frurip, D. J.; McDonald, R. A.; Syverud, A. N. *J. Phys. Chem. Ref. Data* **1985**, *14*, Suppl. 1 (JANAF Tables).
(21) Dagdigian, P. J.; Cruse, H. W.; Zare, R. N. *J. Chem. Phys.* **1975**, *62*, 1824.
(22) Pasternack, L.; Dagdigian, P. J. *J. Chem. Phys.* **1977**, *67*, 3854.
(23) Hildenbrand, J. L. *Chem. Phys. Lett.* **1973**, *20*, 127.
(24) Lias, S. G.; Bartmess, J. E.; Liebman, J. F.; Holmes, J. L.; Levin, R. D.; Mallard, W. G. *J. Phys. Chem. Ref. Data* **1988**, *17*, Suppl. 1.
(25) Pedley, J. B.; Marshall, E. M. *J. Phys. Chem. Ref. Data* **1983**, *12*, 967.
(26) Schamps, J. *J. Chem. Phys.* **1973**, *2*, 352.
(27) Moore, C. E. *Natl. Stand. Ref. Data Ser. Natl. Bur. Stand.* **1970**, *34*.
(28) Ervin, K. M.; Armentrout, P. B. *J. Chem. Phys.* **1985**, *83*, 166.
(29) Schultz, R. H.; Armentrout, P. B. *Int. J. Mass Spectrom. Ion Processes* **1991**, *107*, 29.
(30) Chen, Y.-M.; Clemmer, D. E.; Armentrout, P. B. *J. Chem. Phys.* **1991**, *95*, 1228.
(31) Armentrout, P. B. In *Advances in Gas Phase Ion Chemistry*; Adams, N. G., Babcock, L. M., Eds.; JAI: Greenwich, 1992; Vol. 1, p 83.
(32) Vibrational frequencies for NO_2 are 1357.8, 756.8, and 1665.5 cm^{-1}, for N_2O are 1276.5, 589.2 (2), and 2223.7 cm^{-1}, and for CO_2 are 1384.86, 667.70 (2), and 2349.30 cm^{-1} as given in ref 20.
(33) Gioumousis, G.; Stevenson, D. P. *J. Chem. Phys.* **1958**, *29*, 292.
(34) Calculated from $D°(OAl^+–O) = D°(OAl–O) + IE(AlO) - IE(AlO_2)$ where $D°(OAl–O) = 98.3 \pm 6.5$ kcal/mol and $IE(AlO_2) = 10.5 \pm 1.0$ eV are taken from Ho and Burns, ref 35, and IE(AlO) is taken from Hildenbrand, ref 23.
(35) Ho, P.; Burns, R. P. *High Temp. Sci.* **1980**, *12*, 31.
(36) Armentrout, P. B. In *Structure/Reactivity and Thermochemistry of Ions*; Ausloos, P., Lias, S. G., Eds.; D. Reidel: Dordrecht, 1987; p 97.
(37) Farber, M.; Srivastava, R. D.; Uy, O. M. *J. Chem. Soc., Faraday Trans. 1* **1972**, *68*, 249.
(38) Paule, R. C. *High Temp. Sci.* **1976**, *8*, 257.
(39) Smoes, S.; Drowart, J.; Meyers, C. E. *J. Chem. Thermodyn.* **1976**, *8*, 225.
(40) This value is calculated by explicitly averaging the rotational and vibrational energies assuming Boltzmann distributions (constants from ref 20).
(41) Lessen, D. E.; Asher, R. L.; Brucat, P. J. *J. Chem. Phys.* **1991**, *95*, 1414.
(42) Herzberg, G. *Molecular Spectra and Molecular Structure. III. Electronic Spectra and Electronic Structure of Polyatomic Molecules*; Van Nostrand: New York, 1966.
(43) Troe, V. J.; Wagner, H. G. *Ber. Bunsenges. Phys. Chem.* **1967**, *71*, 946.
(44) Lorquet, A. J.; Lorquet, J. C.; Forst, W. *Chem. Phys.* **1980**, *51*, 253.

Angular Momentum Coupling in Simple-Fission Transition States

Andrew J. Karas and Robert G. Gilbert*

School of Chemistry, University of Sydney, New South Wales 2006, Australia *(Received: August 21, 1992)*

An efficient means is deduced for calculating RRKM microscopic reaction rates for simple-fission transition states by using a Hamiltonian consisting of the separate Hamiltonians for each moiety (A and B), hard-sphere interactions between A and B, and symmetric tops connected by a light rigid rod; the reaction coordinate is the breaking bond. This extension of the simple Gorin model takes exact account of the angular-momentum coupling between A and B and of the transition-state requirement that the density of states of the activated complex be evaluated with the reaction coordinate held fixed. Evaluation for typical systems shows that the simpler treatment where A and B are treated as independent rotors is both accurate and in accord with experiment, if both are small but breaks down when A and/or B are large. In the latter case, the variational calculation gives a rate coefficient that is highly sensitive to the assumed hard-sphere radii; although the model cannot then be used meaningfully for a priori prediction of experiment, it provides a useful means of fitting extant data to predict falloff behavior.

Introduction

The calculation of rate coefficients for reactions proceeding through simple-fission transition states (such as radical–radical recombinations, dissociations, and ion–molecule reactions) is made complex by the fact that some modes (the "transitional" modes) change from vibrations to free rotations along the reaction coordinate from reactant to product. This paper is a contribution to the often-addressed questions of devising a suitable Hamiltonian to describe this situation and devising computational means to describe the dynamics dictated by this Hamiltonian so as to lead to an evaluation of the rate coefficient. Given a form of the Hamiltonian, evaluation of the requisite rate coefficient is usually carried out by using a statistical approach such as RRKM theory or the SACM (for an overview, see, e.g., Gilbert and Smith[1]), employing the basic formula

$$k(E,J) = \frac{W^\dagger(E,J)}{h\rho(E)} \qquad (1)$$

where $k(E,J)$ is the rate coefficient for reaction from a reactant state with energy E and angular momentum, J, $\rho(E)$ is the density of states of reactant, and the sum of states $W^\dagger(E,J)$ is the total number of states that can become product.

RRKM theory starts with the dynamical assumption that there exists a hypersurface in phase space such that all trajectories passing through this hypersurface (defining the transition state or activated complex) from the direction of the reactant valley go on irreversibly to product without recrossing. This model therefore gives an exact upper bound to the exact classical rate coefficient and thus may be used variationally: the transition state can be located as that hypersurface along the reaction coordinate ($r^\dagger$) where the RRKM rate coefficient is a minimum. Practical means of evaluating the RRKM expression for $W^\dagger(E,J)$ may be for simplicity divided into two categories, on the basis of the assumptions made as to the form of the Hamiltonian of this transition state. (1) The first category assumes the Hamiltonian to be separable into harmonic terms for bends, stretches, etc. and separable terms for internal rotations; variants of the direct-count algorithm[1] then enable $W^\dagger(E,J)$ to be evaluated in a few seconds of computer time. The assumed form of the Hamiltonian is readily transferrable: i.e., it can be easily written down for any system and the requisite parameters estimated by straightforward recipes (whose accuracy must of course always be open to question). However, the assumption of a separable Hamiltonian is clearly not an accurate representation of reality: e.g., the fact that the form of the Hamiltonian changes qualitatively between reactant and product (because of the transitional modes) says that the separability assumption cannot generally be valid. (2) The second

* Author to whom correspondence should be sent.

0022-3654/92/2096-10893$03.00/0 © 1992 American Chemical Society